View metadata, citation and similar papers at core.ac.uk

brought to you by CORE

provided by Elsevier - Publisher Connector

Available online at www.sciencedirect.com

SciVerse ScienceDirect

Procedia IUTAM 6 (2013) 114 – 122

Procedia IUTAM

www.elsevier.com/locate/procedia

IUTAM Symposium on Multiscale Problems in Stochastic Mechanics 2012

2D and 3D fracture modeling of asphalt mixture with randomly distributed aggregates and embedded cohesive cracks

Anyi Yin[a], Xinhua Yang[a,] , Zhenjun Yang[b*]

[a]*School of Civil Engineering and Mechanics, Huazhong University of Science and Technology, Wuhan 430074, China*
[b]*School of Mechanical, Aerospace and Civil Engineering, the University of Manchester, M13 9PL, UK*

Abstract

This paper develops a mesoscale finite element method for realistic modeling of complex cohesive fracture in asphalt mixture with a given gradation. A random aggregate generation and packing algorithm is employed to create 2D and 3D heterogeneous asphalt mixture specimens, and cohesive elements with tension/shear softening laws are inserted into both mastic and aggregate-mastic interfaces to simulate crack initiation and propagation. The nucleation and coalescence of microcracks and propagation of macrocracks in 2D and 3D specimens is realistically modeled in detail with a few important conclusions drawn. The effects of coarse aggregate distributions on performance of asphalt mixture are also evaluated.

© 2013 The Authors. Published by Elsevier B.V. Open access under CC BY-NC-ND license.
Selection and/or peer review under responsibility of Karlsruhe Institute of Technology (KIT) Institute of the Engineering Mechanics.

Keywords: asphalt mixture; crcaking; mesoscale modeling; random aggregate generation and packing algorithm; cohesive elements;

* Corresponding author. Tel.: +44 161 3064645E-mail address: zhenjun.yang@manchester.ac.uk

2210-9838 © 2013 The Authors. Published by Elsevier B.V. Open access under CC BY-NC-ND license.
Selection and/or peer review under responsibility of Karlsruhe Institute of Technology (KIT) Institute of the Engineering Mechanics.
doi:10.1016/j.piutam.2013.01.013

1. Introduction

Asphalt mixtures are heterogeneous composite materials comprising irregularly shaped and randomly distributed coarse and fine aggregates, viscous matrix (asphalt) and voids. The complex morphological features at the mesoscale, such as shapes, gradations, distribution and orientation of aggregates, asphalt content and void ratio, directly determine the mechanical properties including fracture resistance. So it is important to develop mesoscale models for analyzing fracture of asphalt mixture. Recently, a number of researchers have been concentrating on the meso and microstructure characteristics of cement like materials and a variety of numerical heterogeneous models are built for numerical representation of random heterogeneity of aggregates in different ways. Numerical image processing technique [1, 2] and parameterization modeling technique [3, 4] are two most popular approaches in explicitly modeling the different material phase in asphalt mixture. However, due to the difficulty of three-dimensional (3D) mesostructure modeling and high computational costs, most of current fracture studies are two-dimensional (2D) models, with few reporting 3D results.

In this study, a heterogeneous fracture modeling approach is developed to simulate complex 2D and 3D crack propagation in asphalt mixture consisting of randomly distributed coarse aggregates and asphalt mastic matrix. In this approach, a random aggregate generation and packing algorithm is devised to create 2D and 3D numerical asphalt mixture samples with heterogeneous mesostructures, and cohesive elements with tension/shear softening are inserted into both the matrix phase and the matrix-aggregate interfaces to simulate crack initiation and propagation.

2. Mesoscale fracture modeling method

2.1. Random aggregate generation and packing algorithm

Table 1 lists a typical aggregate gradation of asphalt mixture. It can be noted that the size of aggregates varies greatly from 16.0mm to 0.075mm. As there usually exist a great number of fine aggregates in asphalt mixture, construction of micromechanical models with a full aggregate gradation is not feasible due to high computational cost. A sensible compromise is to classify the aggregates into coarse and fine aggregates according to the aggregate size. The numerous fine aggregates and asphalt binder are then combined into asphalt mastic, whose mechanical properties are assumed to be uniform. As a result, asphalt mixture is treated as a two-phase material with coarse aggregates embedded in asphalt mastic matrix. The threshold differentiating coarse aggregates (modeled as aggregates) and fine aggregates is, in general, an arbitrary decision, often guided by available computing power and acceptable mesostructure resolution. In 2D studies, 2.36mm is usually taken as the cut-off size of coarse aggregates.

The aggregate generation and packing algorithms proposed by the authors are used to create 2D [5] and 3D [11] numerical asphalt mixture samples with heterogeneous mesostructures here. A number of round (2D) and spherical (3D) aggregates with different sizes are first generated based on a given gradation, then deflated with a defined reduction coefficient and randomly packed into a prescribed region. In order to eliminate conflicts between neighboring aggregates, all reduced aggregates are recovered to their original sizes and relocated by a

Table 1. Full aggregate gradation

Sieve size (mm)	Passing rate (%)
16.0	100
13.2	98.5
9.5	85.4
4.75	63.7
2.36	50
1.18	40.3
0.6	30.2
0.3	20.7
0.15	14.5
0.075	11.3

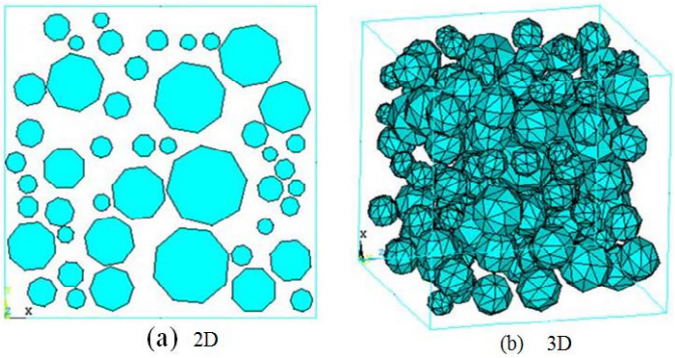

(a) 2D (b) 3D

Fig. 1 Generated samples with randomly distributed aggregates

perturbation process. The round or spherical aggregates are then converted into their corresponding inscribed regular polygons (polyhedron), and a geometrical sample of asphalt mixture is completed. The readers are referred to [5] and [11] for the detailed algorithms.

Fig. 1 (a) and Fig. 1 (b) show typical 2D and 3D examples of asphalt mixture with randomly distributed coarse aggregates, respectively. The 2D aggregates are regular octagons, and the 3D aggregates are polyhedrons with 32 surfaces and 26 vertexes.

2.2. Cohesive interface elements insertion

For 2D specimen models, in order to simulate curved crack paths occurring in asphalt mixture in good accuracy, triangular plane stress elements with constant strain are used to discretize the obtained heterogeneous geometrical models of asphalt mixture. As potential microcrack sources, the 4-node cohesive elements with zero in-plane thickness are inserted into the initial finite element mesh. For 3D specimen model, Tetrahedron solid elements are used and the 6-node cohesive elements with zero out-of-plane thickness are inserted into initial finite element mesh. It is not trivial for inserting cohesive elements into finite element meshes because the arrangement of finite elements is not regular and the amount of them is tremendous. One challenge is how to robustly deal with the changes in the nodal and elemental connectivity due to the insertion of cohesive interface elements. This is tackled by an in-house computer program. The detailed 2D and 3D cohesive element insertion procedures can be found in [6] and [7].

In the mesostructures of asphalt mixture, the potential crack path may traverse through aggregates, mastics, and interfacial surfaces between aggregate and mastic. In general, aggregates are harder to crack than asphalt mastic because of their higher tensile strength. It is assumed in this work that cracking will take place only in asphalt mastic and aggregate-mastic interfaces. The cohesive elements with zero out-of-plane thickness are inserted to represent potential cracks, with different softening laws in the mastic and aggregate-mastic interfaces.

The simple linear tension/shear softening laws [6-7] are used for cohesive elements in this study although more complicated softening laws can be used with ease.

3. 2D Numerical simulation and results

3.1. 2D Numerical analysis model

Based on the gradation in Table 1, a series of 2D numerical asphalt mixture specimens with coarse aggregate cut-off size of 2.36mm are created by using the heterogeneous fracture modeling approach in Section 2. The 2D specimens with dimensions of $50\text{mm}\times 50\text{mm}$ and thickness of 1mm are modeled as plain stress problems under uniaxial tension.

In general, aggregates are linearly elastic, but asphalt mastic is very sensitive to the temperature. It is viscoelastic at higher temperature but brittle and elastic at subzero or very low temperature. Accordingly, asphalt mastic can be regarded as a linearly elastic material approximately at the simulation temperature of -10℃. The material parameters in [8] are used here: E=56.8 GPa, υ=0.15, and ρ=2500 kg/m^2 for aggregates and E=18.2 GPa, υ=0.25, and ρ=2200 kg/m^2 for asphalt mastic, respectively. The cohesive fracture energy G_F= 270 J/m^2 and the tensile strength f_t= 3.78MPa are used for the cohesive elements in mastic, while G_F=77 J/m^2 and f_t=3.44MPa are given for the cohesive elements in the aggregate-mastic interfaces. The initial stiffness 18.2GPa/mm is given for all cohesive elements. Abaqus/Explicit is utilized to solve the highly nonlinear equation systems complicated by softening of cohesive elements and the total loading time for these quasi-static simulations is set as 0.01s. The displacement at the right end increases linearly from 0 to 0.3mm during the loading history.

3.2. Typical crack modes and their evolutions

Two typical types of cracking evolution modes are observed in a group of 2D asphalt mixture specimens under uniaxial tension. The detailed microcrack initiation and propagation processes are presented in Figs 2 and 3 with magnifications of 200 times in (a), (b) and (c) and 5 times in (d), respectively. The split cohesive elements are shown in red to represent microcracks. The red line width indicates the crack width and also represents the energy spent on fracture at the corresponding point of the crack interface. As can be seen from Fig. 2(d) and Fig. 3(d), Type 1 fails with a single main macrocrack and Type 2 with double main macrocracks. Type 1 is often found in the laboratory tensile tests of asphalt mixture, but Type 2 is seldom. Using a 3D high-resolution X-ray scanning technique, the discrete tensile macrocracks very similar to Type 2 were observed in concrete samples in [9].

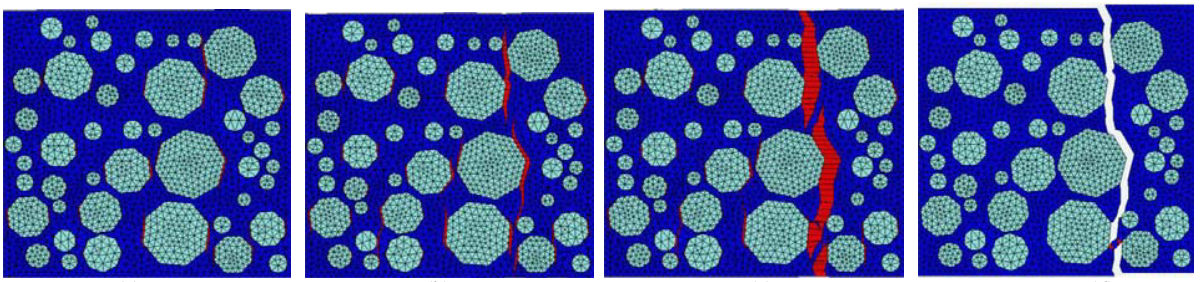

(a) (b) (c) (d)

Fig. 2 Type 1 fracture evolution

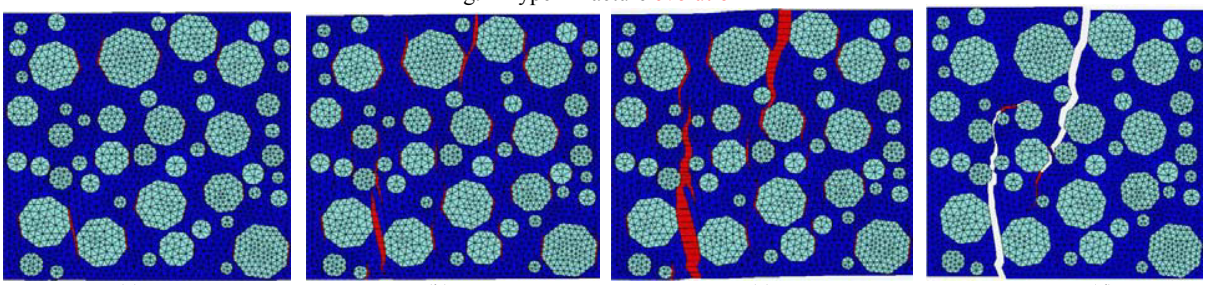

(a) (b) (c) (d)

Fig. 3 Type 2 fracture evolution

In Type 1 fracture evolution, as shown in Fig. 2(a), a number of microcracks are nucleated in the interfaces between aggregates and asphalt mastic in a dispersive manner at very early stage of loading, and their directions are roughly perpendicular to the loading direction. This is often called the interface debonding and can be directly attributed to the weaker material strength of the interface. The similar phenomenon was also observed in a particulate-reinforced material by the optical microscope and the scanning electron microscope in fracture tests [10]. As the displacement increases, the microcracks develop continuously. It is noticeable that the microcracks between two large aggregates grow and coalesce more easily so that a main cracking path gradually forms. The microcracks in the main cracking path grow rapidly and become interconnected, as shown in Fig. 2(b). After the main cracking path is formed, the microcracks in other places are arrested, as shown in Fig. 2(c). After the peak load is reached, the fracture energy is rapidly dissipated while the macrocrack opens further (Fig. 3(d)).

The evolution of the Type 2 fracture is presented in Fig. 3. Similar to the case in Type 1, many microcracks initiate on the aggregate-mastic interfaces randomly at very early stage of loading in Type 2, as shown in Fig. 3(a). As the load increases, the microcracks between two adjacent large aggregates at the top and the bottom grow rapidly, leading to two main cracking paths (Fig. 3(b) and Fig. 3(c)). Finally, two macrocracks form and dissipate a majority of the fracture energy, while the other microcracks are closed as shown in Fig. 3(d).

Both the load and the dissipated fracture energy vs. displacement curves for the fracture modes in Figs 2 and 3 are plotted in Fig. 4. The two fracture types have similar pre-peak responses and very close peak loads (181.842N for Type 1 and 183.463N for Type 2, respectively), but in the post-peak part, the curve for Type 1 has a sharper drop than that for Type 2. Correspondingly, their dissipated fracture energy vs. displacement curves are almost identical in the pre-peak part, but gradually become apart from each other later. At the displacement of 0.3mm, Type 2 fracture mode dissipates about 4.2mJ more energy than Type 1.

It should be noted that the two types of evolution modes, although both are essentially mode-I tensile fracture, represent two fracture mechanisms caused by different distributions of aggregates. In Type 1, the microcracks along the coarse aggregates are merged with little resistance into a single macrocrack, cutting the specimen into two pieces suddenly (Fig. 2). Sometimes two short macrocracks occur with a distance and they do not merge into a single dominant crack as the resistance is high, namely the Type 2 in Fig. 3. The different mechanisms are also reflected by the higher ductility and energy dissipation for Type 2 crack evolution (Fig. 4).

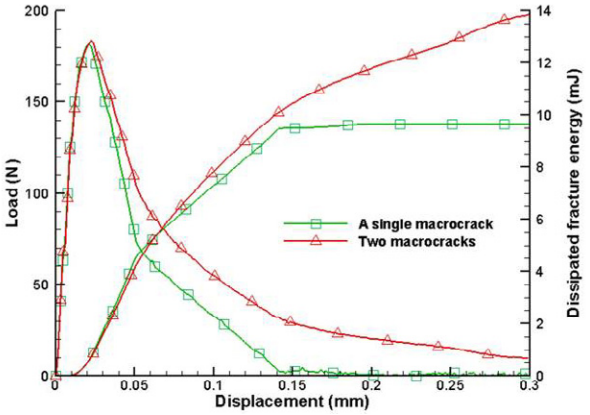

Fig. 4 Load and dissipated fracture energy vs. displacement curves4. 3D Numerical simulation and results

4. 3D Numerical simulation and results

4.1. Crack evolutions in 3D specimens

Moving from 2D to 3D fracture modelling represents a very serious computational challenge because of the dramatic increase of the resources needed due to the considerably increase of elements and nodes. Moreover, for a problem with unknown crack paths, the model needs to be discretized by continuum elements with fine scale in order to minimize the dependence of crack path on the mesh density. So in 3D studies, the numerical asphalt mixture specimens of $50\text{mm} \times 50\text{mm} \times 25\text{mm}$ with larger coarse aggregate cut-off size of 4.75mm are created.

Only one typical crack type, i.e., a single dominant macrocrack, is observed in simulations of a group of 3D asphalt mixture specimens. Fig. 5 illustrates a typical 3D fracture process. The features of microcracks initiation and coalescence and macrocrack propagation in 3D specimens are similar to that observed in 2D specimens.

Figs 6(a-b) show the fracture surfaces of the left and right broken pieces of the numerical specimen in Fig. 5. The gray elements represent asphalt mastic and the green elements represent aggregates. It is found that the fracture surfaces are rough and non-planer and exhibit some bumps and ridges in the through-thickness direction. It can also be observed that most of the cracks are initiated at aggregates-matrix interface, followed by their propagation and merging with others initiating in the mastic matrix near the aggregates. Fig. 6 shows that most of the aggregates (in green) are exposed on the crack surfaces.

A cylindrical specimen directly cored from a pavement is tested in the laboratory at 5℃ under uniaxial tension with loading rate of 1mm/min. The broken surfaces are shown in Fig. 6(c) and (d). It can be seen that the simulated fracture surfaces in Fig. 5 look realistic because all the features of the fracture surfaces described above can be observed in the real fracture surfaces of asphalt mixture.

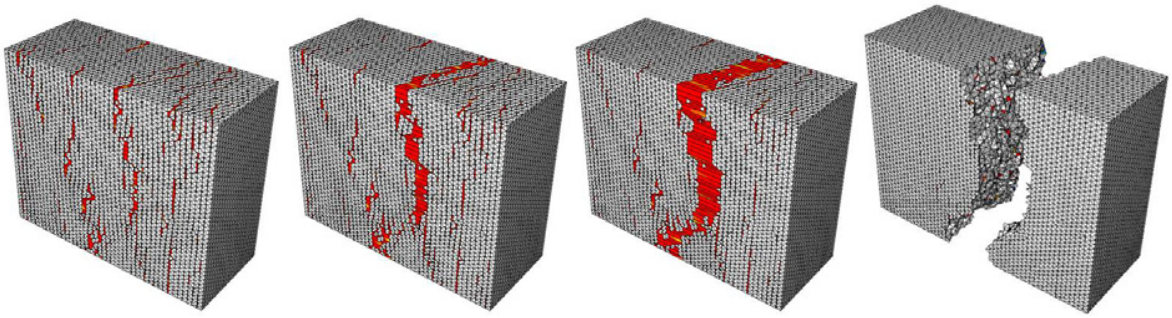

Fig. 5 Crack evolution at different loading stages

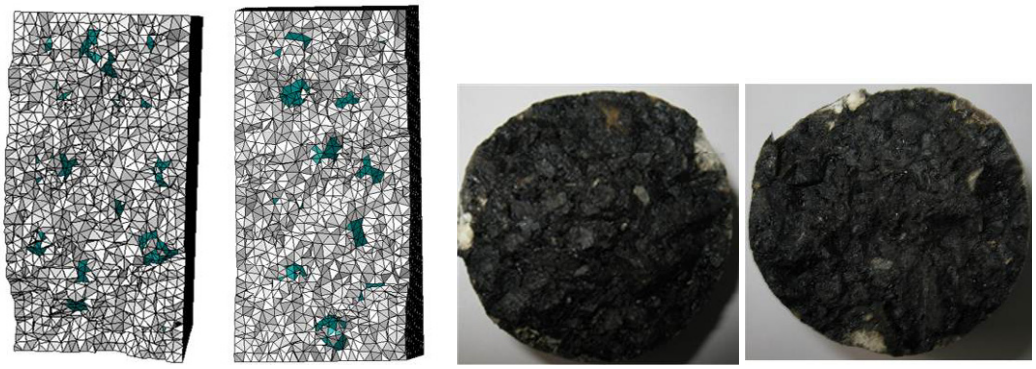

(a) (b) (c) (d)

Fig. 6 Fracture surfaces of a numerical specimen and an experimental specimen

4.2. Effects of coarse aggregate distribution

Fifteen specimens with the same coarse aggregate gradation but different distributions are then modeled. It is found that the predicted crack paths are significantly different. Fig. 7(a) plots the predicted load vs. displacement curves. It can be seen that there is little difference between the predicted pre-peak part and the peak loads (varying from 8,211N to 8,396N with average 8,299N). Some difference exists in the descending softening parts of the curves. These can also be seen on the dissipated fracture energy vs. displacement curves shown in Fig. 7(b). The total dissipated fracture energy predicted ranges from 855mJ to 991mJ with average 921mJ. The energy dissipation is directly attributed to damage evolution and crack propagation. The fluctuation of dissipated fracture energy can reflect the morphological characterization of main macrocrack surface in some degree. The fracture surfaces of the specimens with the minimum and maximum dissipated fracture energy are illustrated in Fig. 8 (a) and (b), respectively. Comparing with the slightly tortuous fracture surface in Fig. 8(a), the fracture surface in Fig. 8(b) is more irregular, tortuous and scraggy, so it has a larger fracture area and thus higher dissipated energy. This has been confirmed by a fractal analysis in [12]. All the crack path, load-carrying capacity and dissipated fracture energy are influenced by coarse aggregate distribution, so a purely deterministic meso-scale model cannot describe the fracture behavior of asphalt mixture very well.

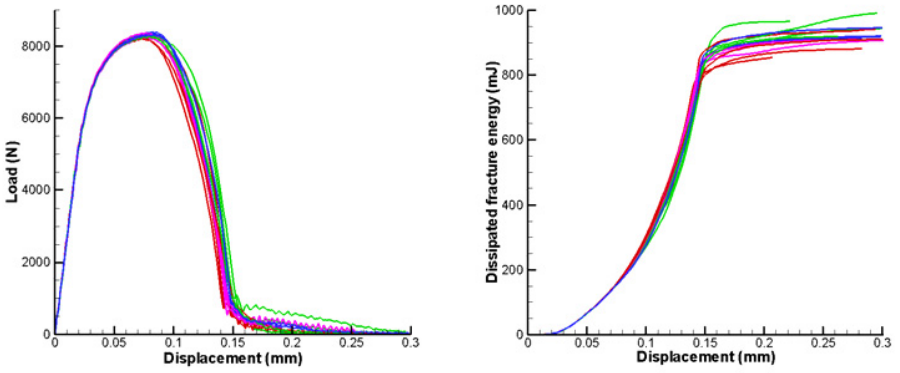

(a) (b)

Fig. 7 Effects of coarse aggregate distribution on the load-carrying capacity and dissipated fracture energy: (a) Load-displacement curves; and (b) Dissipated fracture energy-displacement curves

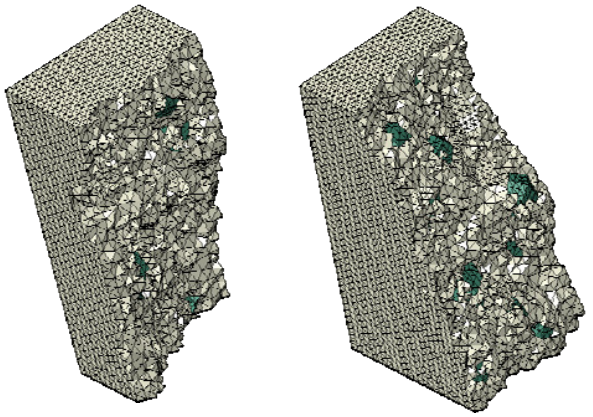

(a) (b)

Fig. 8 Effects of coarse aggregate distribution on the fracture surfaces: (a) dissipated fracture energy 855mJ; and (b) dissipated fracture energy 991mJ

4.3. Comparison of 2D and 3D simulations

To quantitatively compare the load-carrying capacities predicted by 2D and 3D specimens, the averaged load-displacement curves of 15 2D specimens and 15 3D specimens with the same thickness 25mm, the same coarse aggregate gradation and the same coarse aggregate cut-off size 4.75mm are shown in Fig. 9. The averaged peak load for 3D specimens is 8299N, nearly 80% higher than 4566N for 2D. One reason for this increase is that forming of microcracks and macrocracks in 3D specimens is more difficult due to the obstruction of randomly distributed 3D aggregates with many faces and angularity. Another may be the larger area of the unsmooth and non-planar fracture surfaces, which provides higher normal traction [7]. Moreover, the pre-peak range of the averaged load-displacement curve for 3D specimens shows higher nonlinearity than that for 2D specimens.

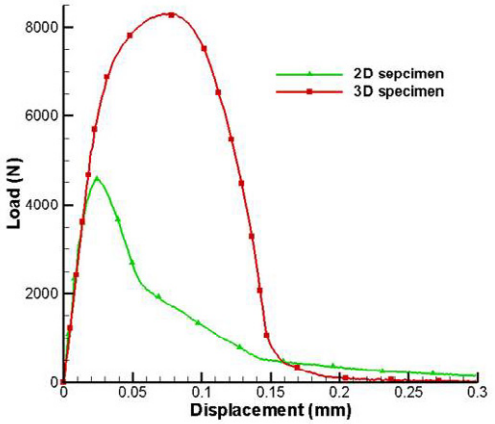

Fig. 9 Comparison of load-carrying capacities between 2D and 3D simulations

5. Conclusions

Important conclusions drawn from this study are: (i) the mesoscale modeling approach is capable of predicting realistic complex crack propagation in asphalt mixture; (ii) the 3D simulations predict more realistic, rougher and non-planar fracture surfaces which are closer to laboratory test observations than 2D simulations; (iii) the microcracks always initiate from the locations at or near aggregate-mastic interfaces in a dispersive manner; (iv) Only a few microcracks dominate the crack propagation and are merged into the macrocrack in growth competition; (v) the dominant cracks basically pass through the area with higher aggregate packing density in 3D specimens; and (v) the coarse aggregate distribution has limited effects on the peak loads but considerable effects on the fracture surfaces and dissipated fracture energy.

Acknowledgements

This work is supported by the National Natural Science Foundation of China (Grant No. 10872073) and National Basic Research Program of China (973 Program: 2011CB013800). ZY would like to acknowledge the support of Alexander von Humboldt Foundation through a Research Fellowship for Experienced Researchers and the State Key Laboratory of Water Resources and Hydropower Engineering Science, Wuhan University, China through an Open Research Grant (No. 2010A004).

References

[1] Dai QL, You ZP. Prediction of creep stiffness of asphalt mixture with micromechanical finite-element and discrete-element models. J Engng Mech-ASCE 2007;**133**:163-73.

[2] Kim H, Buttlar WG. Multi-scale fracture modeling of asphalt composite structures. Compos Sciand Technol 2009; **69**: 2716-23.

[3] Xu R, Yang XH, Yin AY, Yang SF, Ye Y. A three-dimensional aggregate generation and packing algorithm for modeling asphalt mixture with graded aggregates. J Mech 2010; **26**: 165-71.

[4] Yang S F, Yang XH, Yin AY, Jiang W. Three-Dimensional Numerical Evaluation of Influence Factors of Mechanical properties of Asphalt mixture. J Mech 2012; **28**:391-400.

[5] Yin, AY, Yang XH, Yang SF, Jiang W. Multiscale fracture simulation of three-point bending asphalt mixture beam considering material heterogeneity. Engng Fract Mech 2011; **78**: 2414-28.
[6] Yang ZJ, Su XT, Chen, JF, Liu GH. Monte Carlo simulation of complex cohesive fracture in random heterogeneous quasi-brittle materials. Int J Solids Struct 2009; **46**: 3222-34.
[7] Su XT, Yang ZJ, Liu GH. Monte Carlo simulation of complex cohesive fracture in random heterogeneous quasi-brittle materials: A 3D study. Int J Solids Struct 2010; **47**: 2346-45.
[8] Kim H, Buttlar WG. Discrete fracture modeling of asphalt concrete. Int J Solids Struct 2009; **46**, 2593-604.
[9] Landis EN, Nagy EN, Keane DT. Microstructure and fracture in three dimensions. Engng Fract Mech 2003; **70**: 911-925.
[10] Chen ZZ, Tokaji K. Effects of particle size on fatigue crack initiation and small crack growth in SiC particulate-reinforced aluminium alloy composites. Mater Lett 2004; **58**: 2314-21.
[11] Yin, AY, Yang XH, Yang ZJ. 3D fracture modeling of asphalt mixture with randomly distributed aggregates and embedded cohesive zone elements. International Journal of Solids and Structures, under review.
[12] Chang Q, Chen DL, Ru HQ, Yue XY, Yu L, Zhang CP. Three-dimensional fractal analysis of fracture surfaces in titanium-iron particulate reinforced hydroxyapatite composites: Relationship between fracture toughness and fractal dimension. J Mater Sci 2011; **46**: 6118-6123.